

**Design of an Experimental Unit for the Determination of
Oxygen Gas-Liquid Volumetric Mass Transfer Coefficients
using the Dynamic Re-oxygenation Method**

ENE806

Laboratory Feasibility Studies in Environmental Engineering
Spring Semester 2007

Submitted to Dr. Syed A. Hashsham
Department of Civil and Environmental Engineering
A126 Research Complex Engineering
Michigan State University
East Lansing, MI 48824

Dieter Turlousse
&
Farhan Ahmad

Table of Contents

1. Summary	3
2. Introduction	4
3. Experimental Unit	6
3.1 Reactor configuration	6
3.2 Real time data acquisition	10
4. Experimental procedures	12
4.1. Preparation dissolved oxygen sensors	12
4.1.1 Sensor preparation	12
4.1.2 Sensor warm-up	12
4.1.3 Sensor calibration	13
4.1.3.1 Zero dissolved oxygen calibration point	13
4.1.3.2 Saturated dissolved oxygen calibration point	13
4.2. Communication with LabVIEW and data collection	13
5. Experiments	15
5.1. Reactor operating conditions	15
5.2. Determination of the sensor lag constant k_s	16
5.3. Determination of the volumetric mass transfer coefficient $k_{L,a}$	17
6. Results and discussion	19
6.1. Sensor lag constant and effect on $k_{L,a}$ measurements	19
6.2. Volumetric mass transfer coefficient $k_{L,a}$	21
7. Outlook	25
8. References	26
9. Appendix	27

1. Summary

We report on the design and fabrication of an experimental laboratory unit for the determination of the oxygen gas-liquid volumetric mass transfer coefficient $k_{L,a}$ in a bubble column reactor. The total cost of the unit was around \$2,000 and required little or no in-house modification of commercially available items. The reactor was hexagonal in shape and had a column height-to-diameter ratio of 4. Three polarographic sensors were implemented to measure dissolved oxygen concentrations at various axial positions in the water column during oxygen absorption. To illustrate the performance of the experimental unit, the $k_{L,a}$ was determined in distilled water at ambient pressure and temperature. Alongside, factors important in the determination of $k_{L,a}$ in bubble column reactors are discussed and evaluated, with focus on the impact of sensor lag and hydrodynamic conditions in the reactor. It was verified that the estimated $k_{L,a}$ ($\sim 0.31 \text{ min}^{-1}$) was much larger than the sensor lag constant k_s ($\sim 0.16 \text{ s}^{-1}$), thereby justifying the elimination of sensor dynamics in modeling of the re-oxygenation profiles. In addition, it was observed that re-oxygenation profiles were independent of the axial position of the sensors in the reactor, thus allowing implementation of the continuous stirred tank reactor (CSTR) model to estimate $k_{L,a}$. In conclusion, we constructed an experimental laboratory unit for the estimation of $k_{L,a}$ using the dynamic re-oxygenation method using polarographic dissolved oxygen sensors. We provided experimental evidence that the CSTR model without sensor lag can be adopted to extract $k_{L,a}$ values from the measured re-oxygenation profiles.

2. Introduction

Efficient oxygen supply is a principal requirement for all aerobic chemical and biological processes. Aeration refers to the process of addition of oxygen to water by utilization of the principles of mass transfer. In most aerated biological processes, the oxygen transfer rate (OTR) is modeled to be directly proportional to the driving force generated by the difference between the saturation (DO^*) and actual dissolved oxygen concentration (DO) in the liquid phase. The proportionality constant is defined as the volumetric mass transfer coefficient K_La (expressed in reciprocal time units), yielding the following well-known relationship describing oxygen gas-liquid mass transfer:

$$OTR = \frac{d(DO)}{dt} = K_La(DO^* - DO)$$

with DO^* obtained by Henry's law. The K_La is a lumped parameter incorporating the overall resistance to mass transfer and the total specific surface area available for mass transfer:

$$\frac{1}{K_La} = \frac{1}{k_La} + \frac{1}{Hk_Ga}$$

where k_L and k_G represent the liquid and gas phase mass transfer coefficient, respectively, and H the dimensionless Henry constant. In most cases, the liquid phase resistance to mass transfer is dominating and the volumetric mass transfer coefficient is approximated by k_La . The K_La depends on numerous parameters, including liquid phase properties, reactor geometry and operating conditions.

The volumetric mass transfer coefficient k_La is a critical parameter in the design of reactors and aeration systems. During the last decades various techniques for the determination of k_La have been developed (Poughon et al., 2003 and references therein). These methods can be separated into chemical and physical methods (Deront et al., 1998). Chemical absorption methods can be classified depending on the reaction rates

with the sulfite oxidation method being the most widely adopted approach. Physical oxygen absorption methods (based on gassing-in, gassing-out or pressure step) can be dynamic or steady state. In the dynamic gassing-in or re-oxygenation method dissolved oxygen concentration is monitored in the liquid phase during oxygen absorption. Though inherent limitations of the method are well recognized (Gourich et al., 2006), the dynamic re-oxygenation method using dissolved oxygen sensors has been increasingly adopted in current studies on oxygen gas-liquid mass transfer.

A number of factors can confound the measurement of $k_{L,a}$. First, sensor lag can lead to inaccurate dissolved oxygen concentration measurements and inferred $k_{L,a}$ estimates when the characteristic time of the sensor response and re-oxygenation dynamics are of comparable magnitude (Vandu et al., 2004; Gourich et al., 2006). Increased sensor lag leads to reduced estimates of $k_{L,a}$ when this is not considered during modeling of the re-oxygenation dynamics. Second, the hydrodynamic conditions in the reactor and position of the dissolved oxygen sensors are critical for $k_{L,a}$ estimations when perfect mixing is not present (Gourich et al., 2006). Models to extract $k_{L,a}$ from re-oxygenation profiles need to incorporate the hydrodynamics conditions in the reactor if perfect mixing is not present, and spatial gradients exist. This is of particular importance in bubble column reactors where complete mixing is often not obtained.

The goal of this project was to design and build an experimental unit for the measurement of the oxygen gas-liquid volumetric mass transfer coefficient $k_{L,a}$. A bubble column type reactor was selected, and $k_{L,a}$ estimated using the dynamic re-oxygenation method. Polarographic dissolved oxygen sensors were implemented to measure dissolved oxygen concentrations at various axial positions in the water column during oxygen absorption. A series of experiments was performed to test the performance of the experimental unit, with focus on i) determination of the sensor lag constant, and ii) determination of $k_{L,a}$ in distilled water as a demonstration of the developed experimental set-up. In conjunction with this set of experiments a number of assumptions inherent to the estimation of $k_{L,a}$ based on the continuous stirred tank reactor (CSTR) model without sensor lag were evaluated.

3. Experimental Unit

3.1. Reactor configuration

The following section provides an overview of the various components of the experimental unit. All components were commercially available (Table 1), and required little or no modification. Although fabrication of a watertight and user-friendly sensor seal was deemed challenging, we were able to manufacture a straightforward seal using components available in a local hardware store (Home Depot, East Lansing, MI).

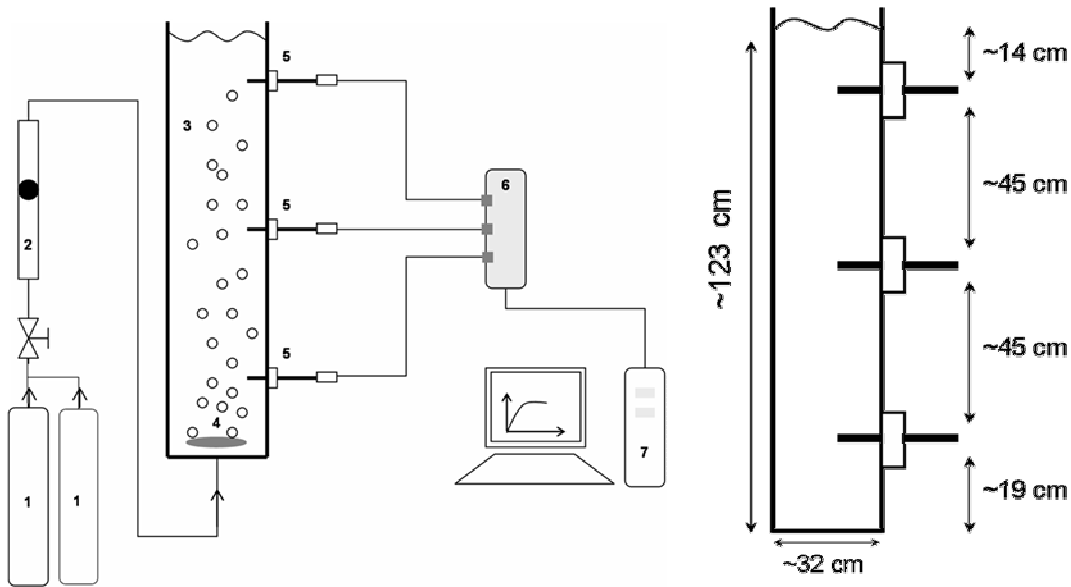


Figure 1. Experimental apparatus. *Left panel.* Major components of the experimental unit: 1, compressed air and nitrogen cylinders connected in parallel; 2, non-calibrated rotameter; 3, bubble column reactor; 4, air diffuser; 5, dissolved oxygen sensors (Vernier, Beaverton, OR); 6, interface (LabPro, Vernier); 7, personal computer equipped with LabView and LoggerPro (30-day demonstration version). *Right panel.* Dimensions of the bubble column (water column height-to-diameter ratio 3.8) and axial positioning of the dissolved oxygen sensors.

Bubble column. The bubble column reactor used in this study was an acrylic hexagonally shaped tower aquarium with a height of 1.27 m and a diameter of 31.8 cm. The tower aquarium was purchased from www.plasticsonline.com at a cost of \$699 excluding shipping costs. Considering the cost of individual acrylic sheets, the option of purchasing an aquarium to serve as bubble column was deemed preferable in comparison with in-

house fabrication. Three holes were carefully drilled in the reactor to accommodate the sensor seal (discussed below). The reactor was filled with water from the top of the reactor using a plastic tube, and emptied rapidly (less than 5 min) by removal of the sensor closed to the bottom of the reactor.

Table 1. Overview and cost of the components of the experimental unit.

Items	Catalog Number	Company	Cost (\$)
Acrylic tower aquarium (50"×12.5")	HT-2	The Billiard Warehouse Inc.	699
Dissolved oxygen sensor	DO-BTA	Vernier Software and Technology	3×199
Vernier LabPro	LABPRO	Vernier Software and Technology	220
Monitor	-----	Panasonic	200
Central processing unit	-----	Colfax	400
Reducing coupling (1/2")	D2466	Home Depot	3×1
Reducer bushing (3/4"×1/2")	438-101	Home Depot	3×1
O-ring washer (3/4")	-----	Home Depot	3×0.5
Gas cylinder (Air & Nitrogen-230 scf)	-----	Linde gas LLC	2×5 per month
Gas regulator, nitrogen (single stage)	CGA-580	AIRCO	100
Gas regulator, air (single stage)	CGA-590	Scott	100
Rotameter	B-250-5	-----	----
Air diffuser (top fin® round airstone, 3")	-----	PetSmart	2.99
Air pump (Stellar S-30)	OE1042	PetSmart	20.99
Chemical resistant tubing, Tygon (2" and 5")	R-3603	Saint-Gobain	30
Glass beaker (600 mL)	FB-2610	KIMAX, USA	5
Glass flask (500 mL)	27060-500	KIMAX, USA	22.06
Glass flask (1 L)	27060-1000	KIMAX, USA	34.82
Magnetic stirrer	M-2200	VMR Scientific	3×98.33
Stirrer bar	SBM5108OTH	STIR BARS	3.50
		Total	\$2,752

Air diffuser. The air diffuser (7.6 cm diameter, Figure 2) used during our initial set of experiments was purchased from a local pet store (PetSmart, East Lansing, MI).

However, it is suggested that for future experiments air diffusers specifically designed for bioreactor aeration should be adopted to yield a better control of the bubble size distribution. The plastic tubing providing air flow to the diffuser was placed in a plastic pipe taped to the reactor wall. The air diffuser was placed under the dissolved oxygen sensors away from the center of the reactor to ensure adequate water circulation in the vicinity of the sensors (Figure 2).

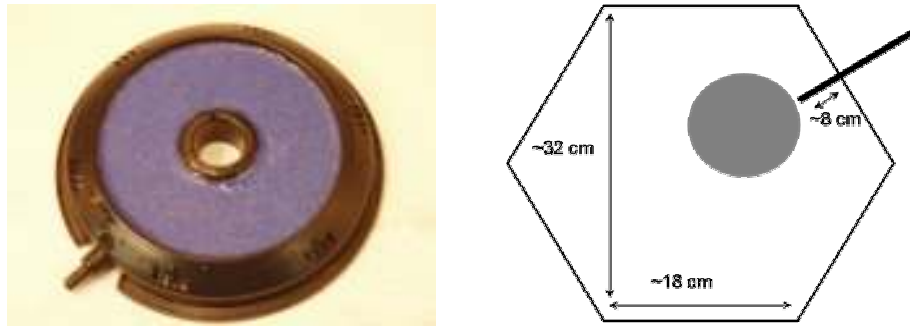
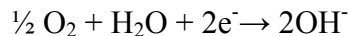


Figure 2. *Left panel.* Air diffuser. *Right panel.* Positioning of the air diffuser with respect to the dissolved oxygen sensor.

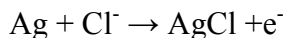
Dissolved oxygen sensors. Three dissolved oxygen sensors were purchased from Vernier Software & Technology (Vernier, Beaverton, OR). The sensors were relatively inexpensive (\$199 per sensor), but it should be recognized that it is recommended by the manufacturer to adopt the sensor for teaching purposes only. It was, however, observed that the sensors performed very well in terms of measurement of changes in dissolved oxygen concentrations, even without calibration. Since estimation of oxygen gas-liquid mass transfer coefficients merely relies upon the rate of changes in dissolved oxygen concentration the sensors were deemed appropriate for our purposes. Adopting the sensors to accurately measure absolute dissolved oxygen concentrations might, however, require additional careful calibration and testing of the sensors.

The Vernier dissolved oxygen sensor is a Clark-type polarographic electrode sensing the dissolved oxygen concentrations in liquid samples. A platinum cathode and Ag/AgCl reference anode in KCl electrolyte are separated from the surrounding sample solution by a oxygen-permeable membrane. A fixed voltage is applied to the platinum electrode,

and oxygen reaching the cathode undergoes the following reduction reaction:



Simultaneously the following reaction occurs at the anode:



As a result, an electric current flows is generated proportional to the dissolved oxygen concentration in the sampled solution. This current is converted to a proportional voltage, amplified, and recorded.

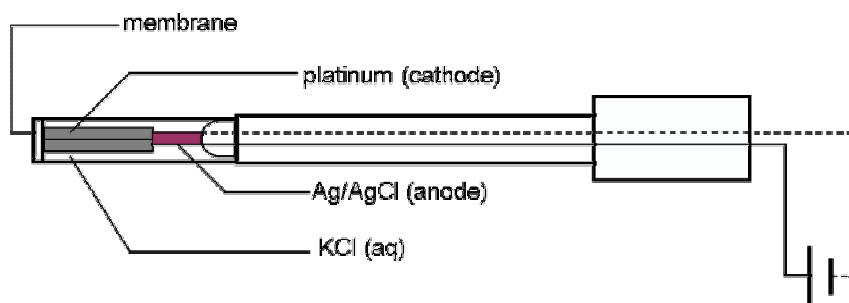


Figure 3. Schematic depiction of the polarographic dissolved oxygen sensor.

Important. *Polarographic dissolved oxygen sensors continuously consume oxygen, and sufficient water flow around the sensor membrane should be ensured to eliminate an apparent drop in dissolved oxygen concentration.*

The sensors were placed across the water column at various axial positions. It was important to reduce potential end effects that might occur if the sensors were placed too close to the bottom of the column where aeration occurs, or too close to the top of the water column. The lower sensor was placed ~19 cm above the bottom of the reactor, and the two other probes were placed ~45 cm apart yielding a distance of ~14 cm between the upper sensor and the level of the water column (Figure 1).

Sensor seal. Design of a seal allowing to readily insert and remove the dissolved oxygen sensors was a critical part of the reactor. We were able to construct a simple sensor seal using items readily available in a hardware store. A detailed view of the seal is presented below along with the dimensions of the various components.

Important. *The threads of the various components (reducing coupling and reducer bushing) purchased from the local hardware store were tapered, and needed to be modified to allow for a tight seal.*

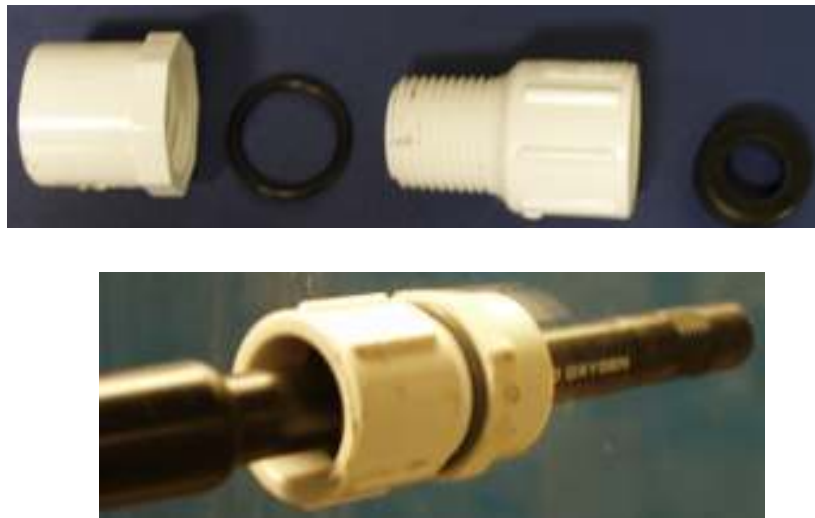


Figure 4. Sensor seal. *Upper panel.* Individual components of the sensor seal. From left to right: reducer bushing ($3/4" \times 1/2"$), O-ring washer ($3/4"$), reducing coupling ($1/2"$), rubber grommet (provided with dissolved oxygen sensors). *Lower panel.* Sensor inserted in seal.

3.2. Real time data acquisition

Data acquisition constitutes sampling of the real world to generate data that can be manipulated by a computer. The components of data acquisition systems (DAS) include sensors to convert the measurement parameter to an electrical signal acquired by the data acquisition hardware. Acquired data is displayed, analyzed, and stored on a personal computer, either using vendor-supplied software, or custom displays. Data acquisition begins with the physical phenomenon or physical property of an object (under investigation) to be measured. This physical property or phenomenon could be the temperature or temperature change of a room, the intensity or intensity change of a light

source, the pressure inside a chamber, the force applied to an object etc. A transducer converts this physical property into a corresponding electrical signal, such as voltage or current. The ability of a data acquisition system to measure different phenomena depends on the transducers to convert the physical phenomena into signals measurable by the data acquisition hardware. DAQ hardware is what usually interfaces between the sensor and a personal computer. It can be in the form of modules that can be connected to the computer's ports (parallel, serial, USB, etc.) or cards connected to slots (PCI, ISA) in a mother board. Driver Software that usually comes with the DAQ hardware or from other vendors, allows the operating system to recognize the DAQ hardware and programs to access the signals being read by the DAQ hardware.

In this experiment a data acquisition interface named LabPro (Vernier Software and Technology) was used. A schematic depiction of the module is presented below (Figure 5). LabPro can be connected to the USB port or serial port of a personal computer. The interface contains two digital and four analog channels for connection of the sensors. LabPro is compatible with LabVIEW, a highly user friendly environment for acquiring, analyzing, displaying, and storing data.

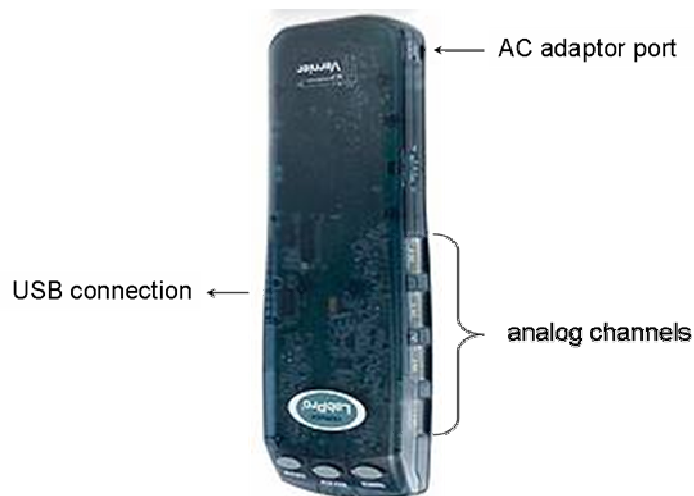


Figure 5. Set-up of LabPro interface for collection of sensor readings.

LabVIEW provides a graphical programming environment highly suitable for data acquisition. LabVIEW programs are called virtual instruments, or VIs, because their

appearance and operation imitate physical instruments. LabVIEW VIs contain the following main components: the front panel, block diagram, and icon/connector. The front panel provides the user an interface for data inputs and outputs. The user operates the front panel by using the computer's keyboard and mouse. Behind the front panel is the block diagram that is responsible for the actual data flow between the inputs and the outputs.

4. Experimental procedures

4.1. Preparation of the dissolved oxygen sensors

The protocol for the preparation, warm-up and calibration of the sensors is discussed below, and the protocol describing both steps can also be found in user's guide provided by the manufacturer (a reprint is provided in the appendix).

4.1.1. Sensor preparation

1. Remove the blue protective cap from the tip of the probe. This protective cap can be discarded once the probe is unpacked.
2. Unscrew the membrane cap from the tip of the probe.
3. Using a pipet, fill the membrane cap with 1 mL of DO electrode filling solution.
4. Carefully thread the membrane cap back on to the electrode.
5. Place the probe into a beaker filled with 100 mL of distilled water.

4.1.2. Sensor warm-up

1. Plug the dissolved oxygen probe into the computer interface and open the LoggerPro or LabVIEW software. The program will automatically identify the dissolved oxygen probe.
2. It is necessary to warm-up the dissolved oxygen probe for 10 minutes before taking readings. To warm up, leave it in water connected with the software for 10 minutes. The probe must stay connected at all times to keep it warmed up. If disconnected for a few minutes, it will be necessary to warm up the probe again.

4.1.3. Sensor calibration

4.1.3.1. Zero dissolved oxygen calibration point

1. Choose 'calibrate' from the experimental menu and click on 'calibrate now' button.
2. Remove the probe from the water and place the tip of the probe into the sodium sulfite calibration solution. (Important: No air bubbles can be trapped below the tip of the probe or probe will sense an inaccurate dissolved oxygen level. If the voltage does not rapidly decrease, tap the side of the bottle with the probe to dislodge any bubbles. The readings should be in the 0.2 to 0.5 V range).
3. Type 0 (the known value in mg/L) in the edit box.
4. When the displayed voltage reading for reading 1 stabilizes (~1 min), click 'keep'.

4.1.3.2. Saturated dissolved oxygen calibration point

1. Rinse the probe with distilled water and gently blot dry.
2. Unscrew the lid of the calibration bottle provided with the probe. Slide the lid and the rubber grommet about 1/2" into the probe body.
3. Add water to the bottle to a depth of 1/4" and screw the bottle into the cap.
4. Type the correct saturated dissolved oxygen value in mg/L (a table with dissolved oxygen saturation values at different temperatures and barometric pressures is provided in the user guide).
5. When the displayed voltage reading for reading 2 stabilizes (reading should be above 2 V), click 'keep' and then 'done'.

4.2. Communication with LabVIEW and data collection

Instrument drivers simplify instrument control and reduce test program development time by eliminating the need to learn the programming protocol for each instrument. An instrument driver is a set of software routines that control a programmable instrument. Each routine corresponds to a programmatic operation such as configuring, reading from, writing to, and triggering the instrument. Use an instrument driver for instrument control when possible. National Instruments provides thousands of instrument drivers for a wide variety of instruments. Use the NI Instrument Driver Finder to search

for and install instrument drivers without leaving the LabVIEW development environment. Select 'Help' to find instrument drivers to launch the 'Instrument Driver Finder'. One can also visit the NI Instrument Driver Network at www.ni.com/idnet to find a driver for an instrument. If a driver is not available for an instrument, you can use the Instrument I/O Assistant Express VI to communicate with the instrument. Before starting to work with LabVIEW download the VIs from www.ni.com and install it on the computer.

The following section provides a step-by-step guide describing the LabVIEW start-up , real time data collection, and storage. Additional information can be found in the user's manuals present in the laboratory.

Step 1. Open LabView and Click to open the user friendly VI program specially designed for measuring real time data.

Step 2. The below presented window (Figure 6) will be displayed which shows the overall block diagram for acquiring data. We have modified the real time measurement VI to acquire the data for all the three probes and saving the data to the specified folder.

Step 3. Wire the resulting signal to either the graph (for waveforms) or the numeric (for scalar values).

Step 4. Configure the Write LabVIEW Measurement File Express VI by double-clicking it and make sure to provide a correct path for the file name.

Step 5. Save the file.

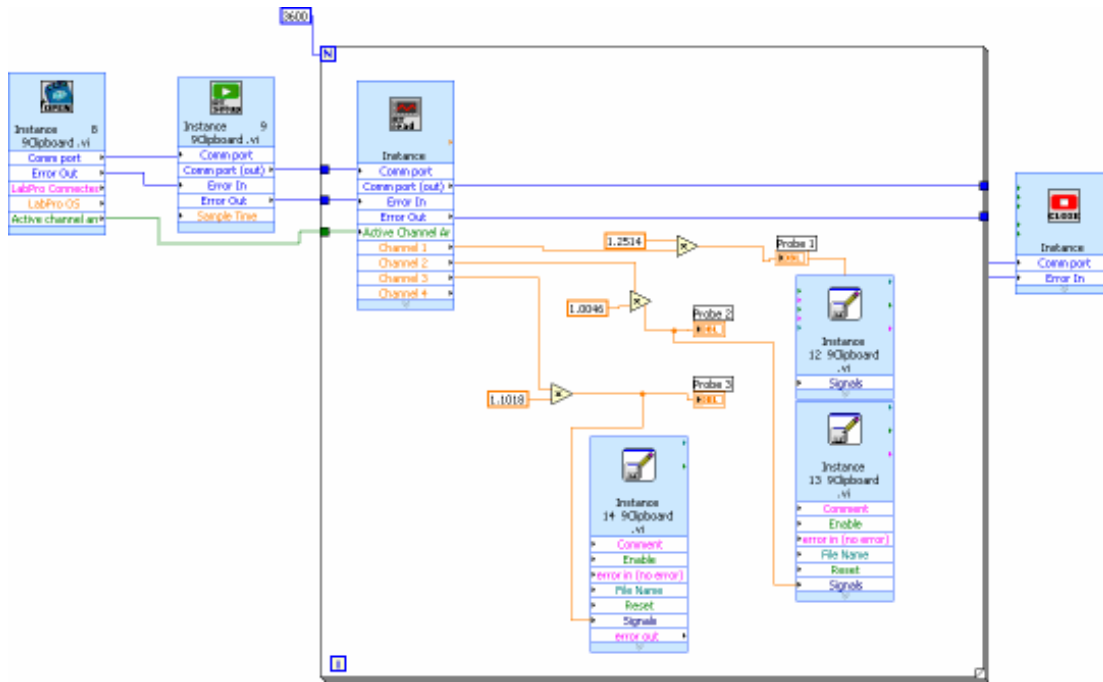


Figure 6. Programmed LabVIEW VI for collection of dissolved oxygen sensor readings.

5. Experiments

5.1. Reactor operating conditions

Reactor operating variables including type of air diffuser, gas flow rate and superficial gas velocity influence the re-oxygenation dynamics and inferred $k_L a$. Hence, knowledge about the operating conditions is vital to accommodate the interpretation of $k_L a$. The liquid phase was in all experiments distilled water, and experiments were performed at ambient temperature and pressure. Table 2 lists a number of reactor operating parameters used during this study as measured by visual inspection. Gas and liquid hold-up were estimated according to the volume expansion method based on measurement of the height of the water column in the presence (H) and absence (H_0) of air bubbles using the following equations:

$$\varepsilon_{gas} = \frac{H - H_0}{H} \quad \text{and} \quad \varepsilon_{liquid} = 1 - \varepsilon_{gas}$$

Superficial gas velocity was estimated by interrupting the gas flow to the reactor and monitoring the time required for the gas bubbles to reach the air-water interface (around 3.5 s). Notwithstanding potential inaccuracies in the measured reactor operating conditions, the provided estimates should be useful in the design of further experiments. However, more advanced methods, such as a high speed camera with dedicated software tools, may be required to measure the superficial gas velocity and bubble size distribution more accurately.

Table 2. Estimated reactor operating conditions.

Parameter	Condition
Superficial gas velocity	~0.3 m/s
Gas hold-up	~0.009
Bubble diameter	~7.5 mm

5.2. Determination of the sensor lag constant

Sensor lag was determined by subjecting the sensors to a near instantaneous alteration in dissolved oxygen concentration, and collecting sensor readings until a constant measurement was observed (Vandu et al., 2004; Philichi and Stenstrom, 1989). The sensor was first equilibrated in a conically shaped beaker (500 mL) continuously sparged with N₂ provided using a gas cylinder. The sensor was then rapidly transferred to a beaker (1000 mL) continuously stirred using a stir bar and magnetic stirrer. The dissolved oxygen concentration was maintained at saturation by continuous sparging of air using an air pump. The sensor dynamics was obtained by monitoring the dissolved oxygen concentration every 0.2 s for a period of 1 min.

***Important.** It should be ensured that no gas build-up exists under the membrane of the sensor. This was achieved by placing the stirrer bar away from the center touching the glass of the flask.*

Sensor lag was assumed to follow a first-order dynamics (Philichi and Stenstrom, 1989;

Letzel et al., 1999; Vandu et al., 2004; Gourich et al., 2006) according to the following equation:

$$\frac{dDO_m}{dt} = k_p(DO_l - DO_m)$$

where DO_m represents the measured dissolved oxygen concentration, DO_l the actual dissolved oxygen concentration, and s_p the sensor lag constant. After integration and linearization this equation yields:

$$\ln\left(\frac{DO_l - DO_m}{DO_l - DO_m^0}\right) = -k_p(t - t_0)$$

with DO_m^0 the initial sensor dissolved oxygen measurement. This equation allows to obtain s_p based on the measured sensor dynamics. The experiment was repeated four times, re-oxygenation profiles from each experiment analyzed separately, and s_p and related parameters reported as the arithmetic mean and standard deviation of the independent determinations.

5.3. Determination of the volumetric mass transfer coefficient

The volumetric mass transfer coefficient k_{LA} was determined using the dynamic oxygen absorption method (Letzel et al., 1999). Dissolved oxygen in the water column was first removed by N_2 sparging until the concentration fell below 1% of the dissolved oxygen concentration at saturation (estimated at 8.66 mg/L at 23 °C and a oxygen partial pressure of 0.21 atm). This step was generally achieved in about 30 min. Oxygen was then introduced in the reactor as compressed air using a diffuser, and the dissolved oxygen concentration monitored during re-oxygenation of the water phase every second until saturation was reached. Switching between nitrogen and air sparging was achieved by opening and closing the main valve of the gas cylinders. The gas cylinder outlet pressure was furthermore adjusted prior to the experiment to yield a constant gas flow as observed using a non-calibrated rotameter (level 11 at the rotameter used during our

experiments). However, this approach did not yield information on the actual air flow, and it is suggested to calibrate the rotameter in order to accurately measure the gas flow rate.

Re-oxygenation profiles were modeled according to the CSTR model without sensor lag:

$$\frac{d(DO)}{dt} = k_L a (DO^* - DO)$$

where DO represents the actual dissolved oxygen concentration in the liquid phase, DO* the dissolved oxygen concentration in equilibrium with the gas phase calculated according to Henry's law, and $k_L a$ the liquid-side volumetric mass transfer coefficient. After integration and linearization this equation can be adopted to obtain $k_L a$ as follows:

$$\ln\left(\frac{DO^* - DO}{DO^* - DO^0}\right) = -k_L a (t - t_0)$$

The experiment was repeated three times, re-oxygenation profiles from each experiment analyzed separately, and $k_L a$ reported as the arithmetic mean and standard deviation of the independent determinations.

6. Results and discussion

The dynamic re-oxygenation method was adopted to assess the gas-liquid volumetric mass transfer coefficient k_La using polarographic sensors to monitor dissolved oxygen concentrations in the water column. The sensor lag dynamics was determined to verify the assumption that sensor lag dynamics was not significant in comparison with re-oxygenation dynamics. The k_La was then estimated for distilled water under ambient pressure and temperature, and the assumption of perfect mixing in the reactor justified.

6.1. Sensor lag constant and effect on k_La measurements

Sensor lag was evaluated by subjecting the sensors to a near instantaneous alteration in dissolved oxygen concentration, and modeling the sensor lag according to a first-order dynamics. A rapid sensor response was observed, and a steady-state measurement was usually observed in less than 30 s (Fig. 7). Sensor lag constants were estimated at 0.18, 0.16, and 0.24 s^{-1} for the different sensors, equivalent to a 95% sensor response time of 16.4, 18.2, and 12.3 s (Table 3). These estimates are in good agreement with Gourich et al. (2006) who determined a sensor lag constant of 0.14 s^{-1} . Vandu and Krishna (2004) observed a sensor lag constant in the order of 0.47 s^{-1} . The determined 95% sensor response time was, however, roughly two times smaller than the response time reported by the manufacturer of the probes.

Table 3. Parameters of sensor lag dynamics (n=4).

Sensor number (axial position, z/d)	k_s (s^{-1})	t_s (s)	t_{95} (s)
1 (0.6)	0.18 ± 0.01	5.6 ± 0.2	16.4 ± 0.5
2 (2.0)	0.16 ± 0.00	6.1 ± 0.1	18.2 ± 0.4
3 (3.4)	0.24 ± 0.00	4.1 ± 0.0	12.3 ± 0.1

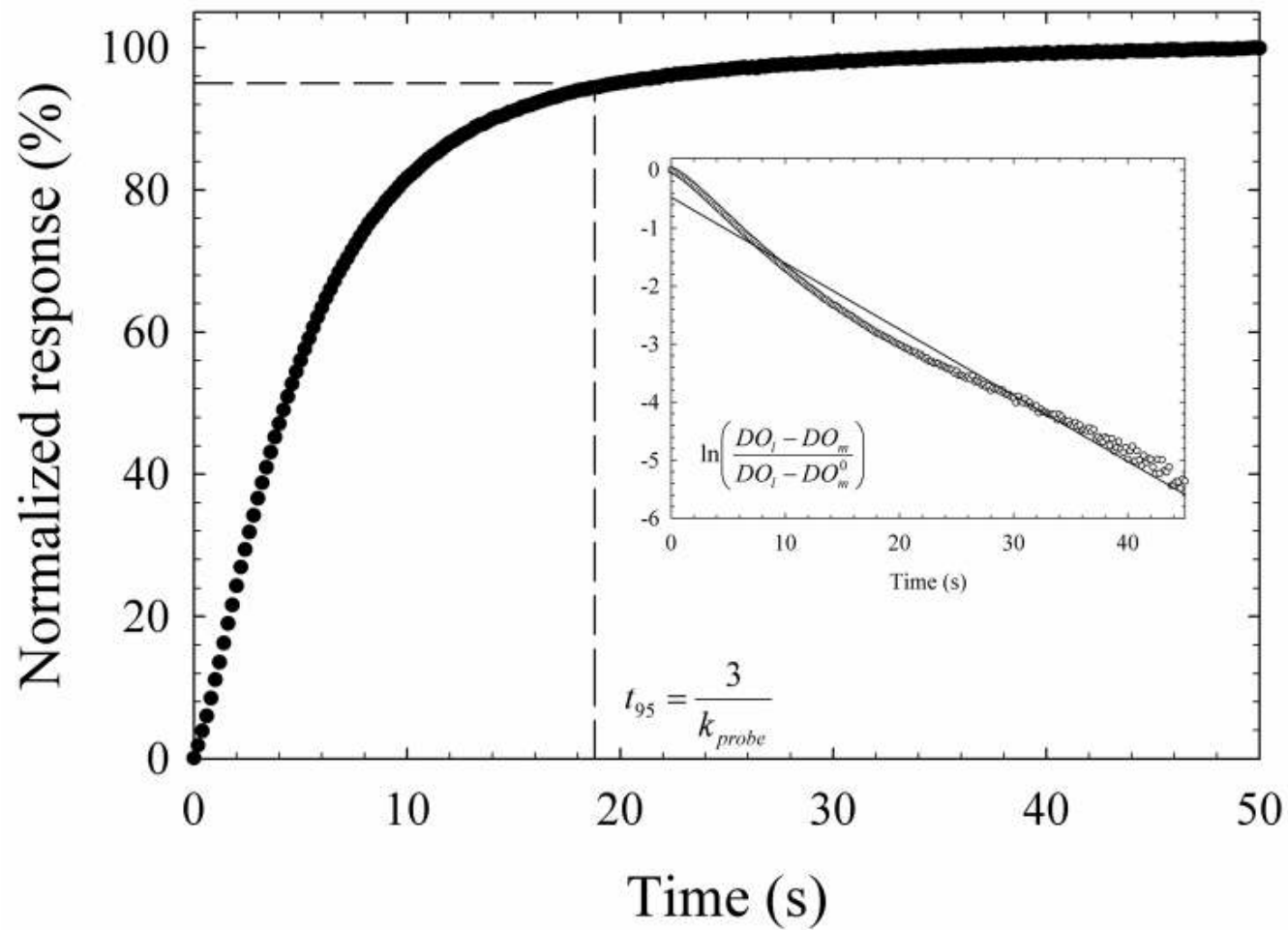


Figure 7. Typical sensor dynamics obtained after a near instantaneous alteration in dissolved oxygen concentration.

Sensor lag can drastically influence the accuracy of dissolved oxygen measurements and inferred $k_{L,a}$ if the characteristic mass transfer time t_m ($1/k_{L,a}$) is similar to the probe response time t_s ($1/k_s$). Philichi and Stenstrom (1989) estimated that the product of the sensor lag constant k_p should be 50 times smaller than $k_{L,a}$ to limit errors in $k_{L,a}$ estimates to less than 1%. Considering that the slowest responding sensor displayed a k_s of 0.16, it was estimated that $k_{L,a}$ values higher than 0.19 min^{-1} could be accurately measured with the sensors used in this project. As demonstrated below, the $k_{L,a}$ observed under the specified reactor operating conditions was higher than this limit, and justified the assumption that sensor lag did not significantly influence $k_{L,a}$ estimates in our experimental set-up.

6.2. Volumetric mass transfer coefficient $k_{L,a}$

The volumetric mass transfer coefficient $k_{L,a}$ was determined using the dynamic re-oxygenation method. Re-oxygenation was initiated by sparging of compressed air using an air diffuser, and complete re-oxygenation was usually observed in less than 20 min (Fig. 8). The linearized plot demonstrated that a mono-exponential process governed the re-oxygenation dynamics, further substantiating the assumption that sensor lag did not noticeably influence the monitoring of the reoxygenation dynamics. Interestingly, overlapping re-oxygenation profiles were obtained for all three sensors at different axial positions with coefficients of variations among the always less than 5% (not shown). The $k_{L,a}$ was estimated at $0.31 \pm 0.01 \text{ min}^{-1}$ expressed as the arithmetic mean and standard deviation of the three independent determinations for all probes (Table 4), translating into a time of 9.79 min to achieve 95% re-oxygenation of the water column.

The CSTR model is the most widely applied method to estimate $k_{L,a}$. This model assumes perfect mixing in both the gas and liquid phase, and constant oxygen concentration in the gas phase. For bubble column reactors with high water column height-to-diameter ratios, however, the axial dispersion (AD) model might be more appropriate to account for non-perfect mixing by incorporation of a dependence of the gas and liquid phase oxygen concentration on the axial position in the column (Han et al., 2007). The latter authors observed that the CSTR and AD model produced different $k_{L,a}$ values, in particular at

positions with increasing distance from the bottom of the reactor expressed as the axial position divided by the diameter of the water column (z/d_c). In this study, no large difference was observed for $k_L a$ estimates at different axial distances (Table 4). This was attributed to the fact that sensor furthest from the bottom of the water column has an axial position of 3.8, and Han et al. (2007) observed that for sensor position-to-column diameter ratios below 3 to 4 the AD and CSTR model yield nearly identical $k_L a$ estimates. This demonstrated that our assumption of ideal mixing was justified, and the BC reactor essentially behaved as a CSTR.

Table 4. Volumetric mass transfer coefficients $k_L a$ (n=3).

Sensor number (axial position, z/d)	$k_L a$ (min^{-1})
1 (0.6)	0.30 ± 0.01
2 (2.0)	0.30 ± 0.00
3 (3.4)	0.32 ± 0.00
Mean	0.31 ± 0.01

The volumetric mass transfer coefficient $k_L a$ in bubble column reactors is dependent on various interrelated parameters, including the gas hold-up ε_{gas} , the superficial gas velocity U_{gas} , and the specific interfacial gas-liquid surface area a . The specific interfacial gas-liquid surface area is related to gas hold-up ε_{gas} and the mean bubble diameter d_b (Wongsuchoto et al., 2003):

$$a = \frac{6\varepsilon_{\text{gas}}}{d_b(1 - \varepsilon_{\text{gas}})}$$

Assuming that the bubbles in reactor possess a uniform diameter of 7.5 mm and a gas hold-up of 0.009 (Table 2), the specific gas-liquid surface area was estimated at 7.2 m^{-1} . This in turn yields an estimated liquid-side mass transfer coefficient k_L of $7 \times 10^{-4} \text{ m/s}$. This estimation is in good agreement with the value of $4 \times 10^{-4} \text{ m/s}$ reported by Painmanakul et al. (2005).

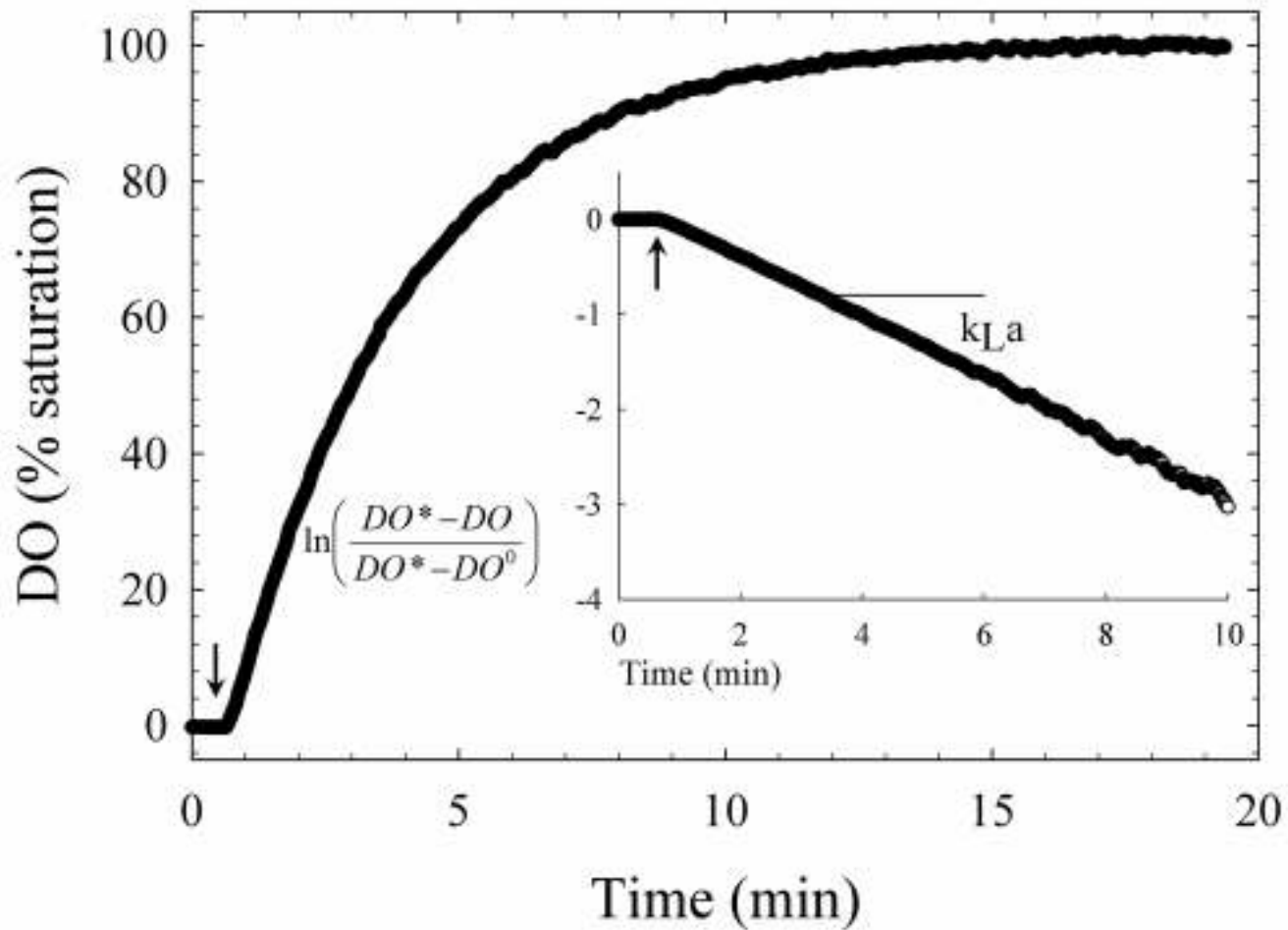


Figure 8. Typical re-oxygenation dynamics. The arrow indicates start of the re-oxygenation process by air diffusion.

The estimated liquid-side mass transfer coefficient in bubble column reactors may vary with superficial gas velocity U_{gas} depending on the range of U_{gas} (Vandu and Krishna, 2004 and references therein). The experiments in this initial study were performed in the so-called churn-turbulent flow regimes ($U_{\text{gas}} \approx 0.3 \text{ m/s} > 0.08 \text{ m/s}$). Vandu and Krishna (2004) previously observed that the volumetric mass transfer coefficient per unit volume ($k_L a / \epsilon_{\text{gas}}$) was independent of U_{gas} for velocities higher than 0.08 m/s. The authors reported a $k_L a / \epsilon_{\text{gas}}$ of 0.48 s^{-1} for a bubble column reactor with a height-to-diameter ratio in the order of 4. This in excellent agreement with the value of 0.57 s^{-1} observed in this study.

7. Outlook

An experimental unit for the determination of volumetric mass transfer coefficient $k_{L,a}$ was designed and fabricated. The developed method adopts dissolved oxygen sensors for monitoring of dissolved oxygen concentration during re-oxygenation of the water column according to the dynamic method. Results obtained from an initial set of experiments demonstrated that sensor lag was sufficiently small and could be ignored during estimation of $k_{L,a}$. In addition, the bubble column reactor behaved similar to a CSTR and no difference in $k_{L,a}$ estimates at various axial positions was observed.

The experimental unit can be adopted to study the effect of various operating conditions, such as superficial gas velocity and bubble size on the volumetric mass transfer coefficient. A number of relevant studies pertaining to the effect of various reactor operating conditions are provided in the references. These and similar studies may serve as the basis for the design of future experiments.

8. References

- Vandu et al. (2004) Volumetric mass transfer coefficient in a slurry bubble column operating in the heterogeneous flow regime. *Chem Eng Sci* 59 (22-23): 5417-5423.
- Han et al. (2007) Gas-liquid mass transfer in a high pressure bubble column reactor with different sparger designs. *Chem Eng Sci* 62 (1-2): 131-139.
- Gourich et al. (2006) Improvement of oxygen mass transfer estimation from oxygen concentration measurements in bubble column reactors. *Chem Eng Sci* 61 (18): 6218-6222
- Vandu and Krishna (2004) Volumetric mass transfer coefficients in slurry bubble columns operating in the churn-turbulent flow regime. *Chem Eng Process* 43 (8): 987-995.
- Philichi and Stenstrom (1989) Effect of dissolved oxygen probe lag on oxygen transfer parameter estimation. *J Water Pollut Control* 61, S3.
- Letzel et al. (1999) Gas holdup and mass transfer in bubble column reactors operated at elevated pressure. *Chem Eng Sci* 54: 2237–2246
- Painmanakul et al. (2005) Effect of surfactants on liquid-side mass transfer coefficients. *Chem Eng Sci* 60 (22): 6480-6491.
- Wongsuchoto et al. (2003) Bubble size distribution and gas–liquid mass transfer in airlift contactors. *Chem Eng Sci* 92: 81–90.
- Data Acquisition Basics Manual, National Instruments, January 1998 Edition.
- Function and VI Reference Manual, National Instruments, January 1998 Edition.

9. Appendix

The appendix contains the following documents:

- Material safety data sheet for sodium sulfite solution
- Material safety data sheet for potassium chloride solution
- Vernier dissolved oxygen sensor user's guide
- Vernier LabPro user's manual
- Dissolved oxygen saturation levels as function of temperature and pressure